are also due to Dr. Todd Schuster at the University of Connecticut for allowing us to use his DG110 stopped-flow fluorometer and for the technical advice that he and John Philo provided. Our thanks to G. Johnson for advice and help with the limping DG110 stopped-flow unit at Yale. Thanks to D. LeMaster for helpful discussions. Our special thanks to Hans Eklund for access to the X-ray coordinates of T4 thioredoxin at the current state of refinement. We acknowledge A. Johnson, T. Mouning, and J. Mouning for their help with manuscript preparation and S. Katti for help with computer graphics.

References

Ananthanaraynan, V. S., & Ahmad, F. (1977) *Can. J. Biochem. 55*, 239–243.

Berglund, O., & Sjöberg, B.-M. (1970) *J. Biol. Chem. 245*, 6030–6035.

Brandts, J. F., Halvorson, H. R., & Brennan, M. (1975) *Biochemistry 14*, 4953–4963.

Brems, D. N., & Havel, H. A. (1989) *Proteins: Struct., Funct., Genet. 5*, 93–95.

Brems, D. N., Plaisted, S. M., Havel, H. A., Kauffman, E. W., Stodola, J. D., Eaton, L. C., & White, R. D. (1985) *Biochemistry 24*, 7662–7668.

Dolgikh, D. A., Abaturov, L. V., Bolotina, I. A., Brazhnikov, E. V., Bychkova, V. E., Gilmanshin, R. I., Lebedev, Yo. O., Semisotnov, G. V., Tiktopulo, E. I., & Ptitsyn, O. B. (1985) *Eur. Biophys. J. 13*, 109–121.

Endo, S., Saito, Y., & Wada, A. (1983) *Anal. Biochem. 131*, 108–120.

Havel, H. A., Kaufman, E. W., Plaisted, S. M., & Brems, D. N. (1986) *Biochemistry 25*, 6533–6538.

Holmgren, A., Söderberg, B.-O., Eklund, H., & Branden, C.-I. (1975) *Proc. Natl. Acad. Sci. U.S.A. 72*, 2305–2309.

Katti, S. K., LeMaster, D. M., & Eklund, H. (1989) *J. Mol. Biol.* (in press).

Kelley, R. F., & Stellwagen, E. (1984) *Biochemistry 23*, 5095–5103.

Kelley, R. F., & Richards, F. M. (1987) *Biochemistry 26*, 6765–6774.

Kelley, R. F., Wilson, J., Bryant, C., & Stellwagen, E. (1986) *Biochemistry 25*, 728–732.

Kuwajima, K., Nitta, K., Yoneyama, M., & Sugai, S. (1976) *J. Mol. Biol. 106*, 359–373.

LeMaster, D. M. (1986) *J. Virol. 59*, 759–760.

LeMaster, D. M., & Richards, F. M. (1988) *Biochemistry 27*, 142–150.

Lin, L.-N., & Brandts, J. F. (1983) *Biochemistry 22*, 553–559.

Mathews, C. R., & Hurle, M. R. (1987) *BioEssays 6*, 254.

Nall, B. T., Gavel, J.-R., & Baldwin, R. L. (1978) *J. Mol. Biol. 118*, 317–330.

Privalov, P. L., Griko, Yu. V., Venyaminov, S. Yu., & Kutyshenko, V. P. (1986) *J. Mol. Biol. 190*, 487–498.

Schmid, F. X. (1981) *Eur. J. Biochem. 114*, 105–109.

Schmid, F. X., & Baldwin, R. L. (1978) *Proc. Natl. Acad. Sci. U.S.A. 75*, 4764–4768.

Shalongo, W., Ledger, R., Jagannadham, M. V., & Stellwagen, E. (1987) *Biochemistry 26*, 3135–3141.

Söderberg, B.-O., Sjöberg, B.-M., Sonnerstam, U., & Branden, C.-I. (1978) *Proc. Natl. Acad. Sci. U.S.A. 75*, 5827–5830.

Utiyama, H., & Baldwin, R. L. (1986) *Methods Enzymol. 131*, 51–70.

Wong, K. P., & Tanford, Ch. (1973) *J. Biol. Chem. 248*, 8518–8523.

Pulsed Electron Paramagnetic Resonance Studies of the Interaction of Mg-ATP and D_2O with the Iron Protein of Nitrogenase†

T. V. Morgan,‡ J. McCracken,§ W. H. Orme-Johnson,‖ W. B. Mims,⊥ L. E. Mortenson,*,‡ and J. Peisach§

University of Georgia, Center for Metalloenzyme Studies, Athens, Georgia 30602, Department of Molecular Pharmacology, Albert Einstein College of Medicine, Bronx, New York 10461, Department of Chemistry, Massachusetts Institute of Technology, Cambridge, Massachusetts 02139, and Consultant, Exxon Research and Engineering Company, Annandale, New Jersey 08801

Received October 26, 1989

ABSTRACT: Mg-ATP binds to the iron protein component of nitrogenase. The magnetic field dependence of the linear electric field effect (LEFE) in pulsed EPR is consistent with a single 4Fe-4S cluster. The LEFE is virtually unaltered when Mg-ATP is bound. Electron spin echo envelope modulation techniques were employed to evaluate the possibility of a magnetic interaction between ^{31}P of Mg-ATP and the Fe-S center of the iron protein. None was detected. However, weak modulations possibly attributable to peptide ^{14}N were seen, and these were slightly shifted by Mg-ATP addition. Further, protons in the vicinity of the Fe-S cluster of the protein readily exchange with D_2O, and this process is unaffected by Mg-ATP.

Nitrogenase catalyzes the reduction of dinitrogen to ammonia (Burgess, 1984; Orme-Johnson, 1985). It can be separated into two components, one an iron–sulfur protein here termed the iron protein, consisting of two equivalent 30-kDa subunits, and a larger protein containing an iron–molybdenum cofactor (Nakos & Mortenson, 1971). The current view is that the iron–sulfur protein contains a 4Fe-4S cluster bound at an interface between both subunits (Anderson & Howard, 1984). Enzyme catalysis depends on the transfer of electrons by the reduced iron–sulfur protein to the iron–molybdenum protein, concurrent with hydrolysis of bound Mg-ATP (Thorneley et al., 1979).

† This work was supported by U.S. Public Health Service Grants GM 40067-02 to L.E.M. and GM 40168 and RR 02583 to J.P.

‡ University of Georgia.
§ Albert Einstein College of Medicine.
‖ Massachusetts Institute of Technology.
⊥ Exxon Research and Engineering Company.

0006-2960/90/0429-3077$02.50/0

When Mg-ATP is bound to the iron–sulfur protein, the E_m is lowered from about −280 to −430 mV (Zumft et al., 1973), oxygen sensitivity is increased and the iron atoms become accessible to metal chelators (Walker & Mortenson, 1973). In addition, the rhombic EPR spectrum of the reduced protein (Orme-Johnson et al., 1972; Zumft et al., 1974) becomes more axial, and the circular dichroism spectrum undergoes changes as well (Stephens et al., 1979). The effects of Mg-ATP binding suggest a protein conformational change, but no information is available to indicate whether direct interaction between the iron–sulfur center and Mg-ATP occurs. Further, the reasons for increased sensitivity to metal chelators, such as greater access to solvent, are poorly understood.

For these reasons, we have undertaken a pulsed EPR study of the iron protein of nitrogenase from both *Azotobacter vinelandii* and *Clostridium pasteurianum*, specifically addressing the effects of Mg-ATP binding on site symmetry as probed by the LEFE[1] in EPR. With ESEEM spectroscopy, we attempt to ascertain whether ATP bound to the protein is proximate to the iron–sulfur center. In addition, we address possible alteration in the accessibility of the iron–sulfur cluster to solvent protons brought about by Mg-ATP binding, as assessed from ESEEM comparisons of the reduced protein exchanged against D_2O.

Methods

C. pasteurianum and *A. vinelandii* were harvested from log-phase 300-L cultures grown on minimal salt media plus sugar. *C. pasteurianum* nitrogenase was purified by a modification of the method of Mortenson (1972), while *A. vinelandii* nitrogenase was purified according to the method of Burgess et al. (1980). Protein concentration was determined by the Lowry method (Lowry et al., 1951).

All purification procedures were carried out in the absence of O_2 by using Ar-equilibrated buffers containing 1 mM sodium dithionite. All studies were done in 50 mM Tris-HCl, pH 8.0, buffer. TRIZMA-premixed 50 mM Tris/Tris-HCl buffer, pD 8.3, was used for D_2O experiments. Protein samples in quartz EPR tubes and in pulsed EPR cavities (see below) were prepared under argon, either in a Vacuum Atmospheres glovebox or in an anaerobic container.

D_2O exchange of protein samples was carried out by an initial 5-fold concentration of protein solutions under argon using a PM-30 membrane in a microconcentration cell (Amicon), followed by dilution with anaerobic D_2O buffer, pD 8.3, to 80% D_2O concentration. The minimum elapsed time between dilution of protein to freezing of samples in EPR tubes, under anaerobic conditions, was 15 s.

Continuous wave EPR spectral characterization of reduced protein samples was carried out on a Bruker ER300Δ spectrometer at 12 K. Pulsed EPR experiments were performed at liquid He temperature with a spectrometer described elsewhere (McCracken et al., 1987). LEFE measurements were made as described by Mims (1974). Anaerobic samples were transferred with a hypodermic syringe into the LEFE cavity resting in an anaerobic chamber, partially fabricated from brass. The chamber had a clear plastic cover which was fitted with a rubber septum stopper. Prior to protein transfer, the chamber was made O_2 free by evacuating and then filling with highly purified Ar at least five times. Once the cavity was filled, the chamber was immersed in liquid N_2 until visual examination showed that the sample was frozen. The chamber was then opened and the cavity quickly immersed in liquid N_2. Excess sample that protruded above the dipole resonator in the cavity (Mims & Peisach, 1976b, Figure 1) upon cooling was scraped off with a metal blade, leaving prisms of samples, each approximatey 5 × 5 × 2 mm, between the electrode and the walls of the cavity.

The electric field shift parameter (Peisach & Mims, 1973), σ, is defined by

$$\sigma = d/[6f(\tau V)_{1/2}]$$

where d is the thickness of the sample, f is the microwave frequency, and $(\tau V)_{1/2}$ is the product of the applied electric field pulse voltage and τ, the microwave pulse spacing, required to produce a 50% reduction in spin echo amplitude. The shift parameter σ is related to the mean fractional shift in g, $(\delta g/g)_{av}$, per unit of applied electric field, E. Data were collected at increments of magnetic field that encompassed the EPR absorption envelope of the paramagnetic species under investigation.

ESEEM measurements were made on samples directly contained in the same stripline cavity used for LEFE measurements (Mims & Peisach, 1976b) or alternatively in a quartz EPR tube using a reflection cavity described by Britt and Klein (1987) that employs a folded stripline (Lin et al., 1985) as the resonant element. Data were collected by using two-pulse and three-pulse, or "stimulated echo", methods (Hahn, 1980). For three-pulse studies, values of τ were chosen to suppress the proton frequency (Mims, 1972a; Mims & Peisach, 1981). ESEEM spectra were obtained by Fourier transformation using the dead-time reconstruction technique described by Mims (1984).

Results and Discussion

LEFE. Studies of the magnetic field dependence of the LEFE, i.e., of the way in which the electric field induced shifts vary for different settings in the EPR spectrum, have proven useful in determining the number of metal atoms that constitute the paramagnetic polynuclear cluster in an iron–sulfur protein (Peisach et al., 1983). An advantage of this method is that determination of the type of cluster type does not depend on extrusion methods (Berg & Holm, 1982) which may yield equivocal results. In Figure 1 (upper panels) we show the magnetic field dependence of the LEFE for the isolated iron proteins of *A. vinelandii* and *C. pasteurianum* nitrogenase. The curves have the same form as those observed for the four-iron ferredoxin from *Clostridium acid-urici* though the shift magnitudes are 1.5–2 times greater, and do not resemble those obtained for two-iron or three-iron ferredoxins. It is concluded from these studies that the iron–sulfur centers in each Fe protein contain four iron atoms in a single cluster, as had been previously suggested by magnetic circular dichroism, EXAFS, Mössbauer, and preliminary LEFE studies (Stephens et al., 1982; Smith & Lang, 1974; Gillum et al., 1977; Orme-Johnson et al., 1977).

The LEFE results, in conjunction with EPR data, also lead to some conclusions regarding the symmetry properties of the unpaired electron in the iron–sulfur cluster. Were the electron to be distributed equally among the four Fe atoms in an ideal cubane site (Peisach et al., 1977), it would have T_d point symmetry, and a single isotropic g value would be observed in the EPR. Since there are at least two g values, this symmetry must therefore be lowered, either by spontaneous distortion of the cubane structure or by contributions to the ligand field arising from groups outside the structure.

If an axial g tensor were to result from the lowering of the cubane symmetry to D_{2d}, as is found for the Mg-ATP complex

[1] Abbreviations: LEFE, linear electric field effect; ESEEM, electron spin echo envelope modulation.

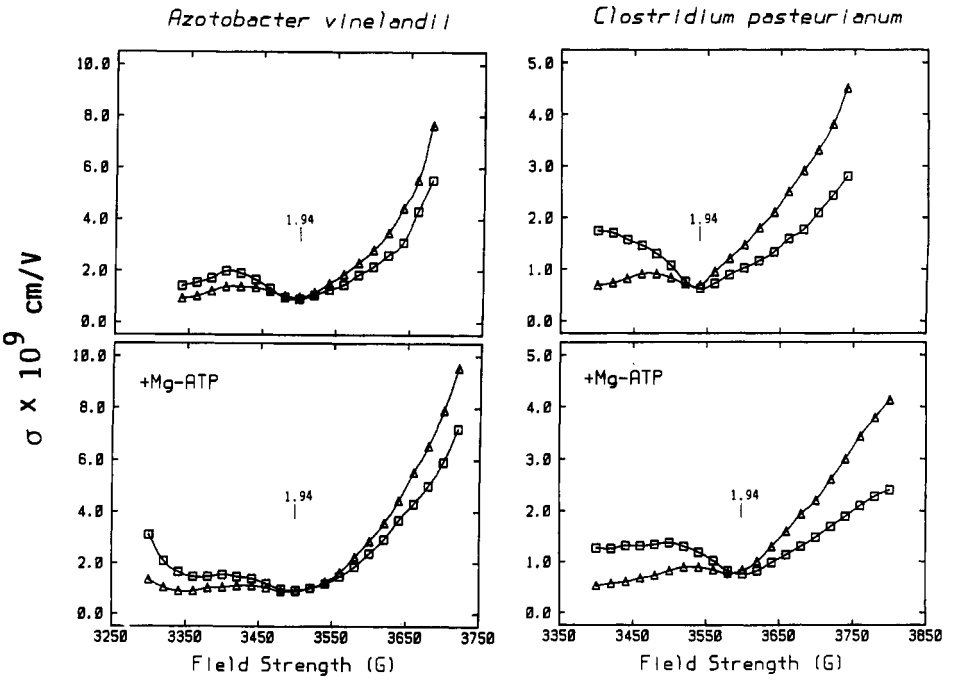

FIGURE 1: Magnetic dependence of the LEFE for the nitrogenase Fe proteins of *A. vinelandii* (left column) and *C. pasteurianum* (right column) in the absence (upper panels) and presence (lower panels) of Mg-ATP studied at 4.2 K. (△) Data collected with $E_{\perp}H$; (□) data collected with $E_{\parallel}H$. Measurement conditions were, for *A. vinelandii* protein, microwave frequency, 9.48 GHz; τ, 700 ns; sample thickness, 0.198 cm. Measurement conditions were, for *C. pasteurianum* protein, microwave frequency, 9.61 (upper panel) and 9.77 GHz (lower panel); τ, 600 ns; sample thickness, 0.193 cm.

of the iron protein, the electron still being shared equally among the four Fe atoms, then it can be shown by computer simulation that the LEFE curves would be quite unlike those seen here (Figure 1, lower panels). For D_{2d} symmetry, for example, the $E_{\parallel}H_0$ and $E_{\perp}H_0$ shifts would fall to zero at the two ends of the EPR spectrum (Peisach & Mims, 1976, Figure 1).[2] In contrast with this, the curves shown in Figure 1 of the present work are characterized by a rise in the shifts at one or at both ends of the EPR spectrum, with the $E_{\parallel}H_0$ shift greater than the $E_{\perp}H_0$ shift at the g_{max} end, and the $E_{\perp}H_0$ shift greater than the $E_{\parallel}H_0$ shift at the g_{min} end. This type of behavior is seen in cases where there is a strong axial component of the odd ligand field lying in the same general direction as the g_{max} axis. [See, for example, the curves obtained for some low-spin heme compounds (Mims & Peisach, 1976a).] It should be noted that these conclusions refer to the symmetry of the paramagnetic center and do not contradict the result of Mössbauer studies (Dickson & Cammack, 1974; Thompson et al., 1974), which indicate delocalization of the electron in the four-iron complex. However, they do strongly suggest that the electron wave function is polarized by groups outside the cubane structure and is not distributed equally over the four Fe atoms.

In the absence of Mg-ATP, the axial symmetry of the metal clusters in the reduced iron protein is lowered to rhombic and the EPR line shape undergoes a significant change (Orme-Johnson et al., 1972; Zumft et al., 1974). This is not accompanied by any major qualitative change in the form of the LEFE curves which still indicate the presence of a four-iron cluster. The overall magnitudes of the shifts are also not greatly altered. A result of this kind is consistent with the view that in the absence of Mg-ATP there is a new component to the odd ligand field, a component that is smaller than those already present but still of a significant amplitude.[3] These findings do not indicate whether the Mg-ATP effect is al-

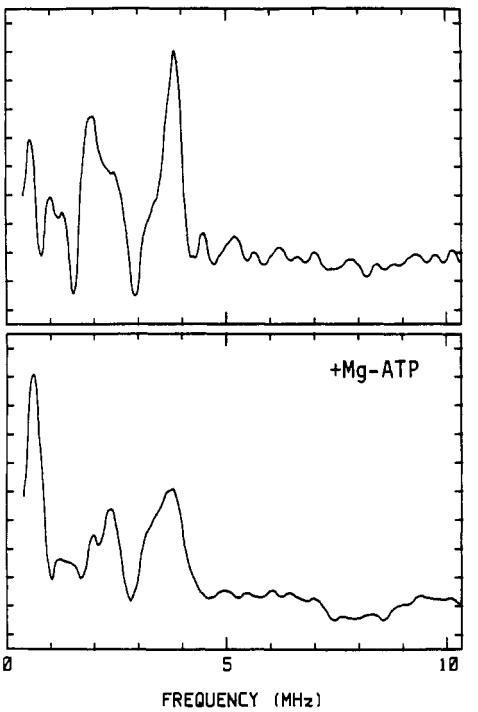

FIGURE 2: Three-pulse ESEEM spectra obtained for *A. vinelandii* iron protein in the absence (upper panel) and presence (lower panel) of Mg-ATP. Measurement conditions were microwave frequency, 9.4 GHz; magnetic field strength, 3460 G; microwave pulse power 30 W (20-ns FWHM); sample temperature, 1.8 K; τ, 135 ns; and pulse repetition rate, 200 Hz; each point represents the average of 60 events.

[2] For simulations that do not involve hyperfine structure, see Figure 6 in Mims and Peisach (1976a); the relevant parameters for D_{2d} symmetry are B_{14}, B_{25}, B_{36}.

[3] Unfortunately, no comparable example can be cited from the biological literature. Studies of paramagnetic centers in inorganic host lattices, with and without nonmagnetic charged ions in the neighborhood, have also shown major changes in the g tensor in conjunction with small changes in the LEFE magnitudes (Mims & Gillen, 1967).

losteric or proximate. The ESEEM experiments distinguish between these two possibilities.

ESEEM. Three-pulse ESEEM data taken at 9.4 GHz for the *A. vinelandii* iron protein show shallow, low-frequency modulations that give rise to frequency components at 0.6, 1.2, 2.2, and 3.8 MHz in the Fourier transforms. For data collected at $g = 1.94$ (Figure 2, upper panel), all four components are observed, while at $g = 1.86$ (data not shown), the higher frequency component shifts to 3.9 MHz and dominates the ESEEM spectra.

Similar ESEEM spectra were obtained for samples treated with Mg-ATP. At $g = 1.94$ (Figure 2, lower panel), three frequency components at 0.6, 2.2, and 3.7 MHz were resolved. Three spectral features were also observed at $g = 1.86$, but with frequencies shifted to ~1.0, 2.4, and 3.8 MHz. ESEEM experiments were also performed at 8.8 and 10.0 GHz on the Mg-ATP-treated protein with only small shifts of ±0.1 MHz being observed for the resolved low-frequency modulation components. The spectral lines observed in all cases are consistent with their assignment to ^{14}N.

Weak magnetic couplings between Fe-S clusters and ^{14}N have been observed for beef heart succinate dehydrogenase, spinach ferredoxin, *Saccharomyces platensis proteolytica* ferredoxin, and *Escherichia coli* fumarate reductase (LoBrutto et al., 1987; Cammack et al., 1988). X-ray crystallographic studies of *S. platensis proteolytica* ferredoxin (Tsukihara et al., 1981) suggest that the weakly coupled ^{14}N frequencies detected in ESEEM studies likely arise from peptide nitrogens involved in NH···S type hydrogen bonding to the Fe-S cluster (LoBrotto et al., 1987). An analysis of similar low-frequency ESEEM data found for Fe-S center 2 of *E. coli* fumarate reductase yielded magnetic coupling constants consistent with such an assignment (Cammack et al., 1988). This work also showed that as the superhyperfine splittings are, for the most part, determined by the ^{14}N nuclear quadrupolar interactions, the observed modulation frequencies are somewhat insensitive to the effective g value at which the ESEEM experiment is carried out.

In contrast, the relative amplitudes of the ESEEM lines change markedly as a function of g_{eff}. In general, these relative amplitudes are expected to depend on the g value of the measurement, the relative orientation of the hyperfine and nuclear quadrupole coupling tensors with respect to the g tensor, and the τ value for three-pulse, or stimulated echo, study (Mims, 1972a,b). For the ESEEM data collected for the iron–sulfur cluster of *A. vinelandii* iron protein, only slight shifts in ^{14}N frequencies due to Mg-ATP addition were seen. However, for data taken under identical resonance conditions (Figure 2) the relative peak amplitudes differ significantly. These differences may indicate a change in structure as it relates to the coupling between the Fe-S cluster and the ^{14}N nucleus giving rise to the ESEEM. Unfortunately, the ^{14}N modulation depths observed for the iron–sulfur clusters of the *A. vinelandii* and *C. pasteurianum* proteins are too shallow at X-band to allow further analysis. A more detailed understanding of these structural changes awaits investigations to be carried out at lower microwave frequencies, where data amenable for a more thorough treatment will likely be obtained (Flanagan & Singel, 1987).

ESEEM measurements carried out on Fe proteins from both *A. vinelandii* and *C. pasteurianum* in the presence of Mg-ATP provided no evidence for ^{31}P coupling to the Fe-S cluster. For weakly coupled phosphorus, one would expect a peak at the larmor frequency of ^{31}P (~6.0 MHz for the conditions used for the measurements of Figure 2) or, were the magnetic coupling stronger, a pair of lines centered at approximately the ^{31}P larmor frequency and split by the electron–nuclear hyperfine coupling energy would be seen. Also, the ESEEM frequencies arising from ^{31}P hyperfine coupling would show a much more pronounced dependence on magnetic field strength than is observed.

The failure to detect ^{31}P ESEEM for the Fe proteins with Mg-ATP is noteworthy and prompted further investigations aimed at determining the limits for detecting ^{31}P superhyperfine coupling at X-band by use of the ESEEM technique. These investigations were based on computer simulations of ESEEM spectra that were made by using the standard density matrix formalism developed by Mims (1972a,b) and also with an orientation averaging scheme developed for ENDOR analysis of randomly oriented transition metal species (Hurst et al., 1985). The modulation depths depend critically on the relative values of the nuclear Zeeman and electron–nuclear superhyperfine coupling energies. For the X-band resonance conditions used for these studies, the nuclear Zeeman frequency of ^{31}P is ~6.0 MHz. If the electron–nuclear hyperfine tensor is taken as axial and the anisotropy is modeled by using the point dipole–dipole approximation, one finds that if the isotropic part of the tensor, A_{iso}, is set to zero, a dipole–dipole distance of 3.0 Å or less would be required to obtain modulation depths greater than 2% of the spin echo intensity, the approximate noise level of our measurements. As the value of A_{iso} is increased, the maximum dipole–dipole distance increases as well. When the value of A_{iso} approaches twice the ^{31}P larmor frequency, the modulation component that arises from the electron spin manifold where nuclear Zeeman and hyperfine terms nearly cancel one another becomes large. For $A_{iso} = 10$ MHz, a dipole–dipole distance of 6.0 Å will yield modulation depths of ~8% at $g = 1.98$. These results suggest that the absence of ^{31}P ESEEM for iron protein in the presence of Mg-ATP likely indicates that the phosphate of ATP is not bound to the Fe-S cluster. This conclusion is in accord with the finding that although the EPR line shape is altered by Mg-ATP binding, the average g value, 1.97, taken as an indicator of metal ligand structure (Blumberg & Peisach, 1974), is not affected.

Water Accessibility. Although the Fe-S cluster has EPR and LEFE properties resembling those of a number of 4Fe-4S proteins, there is a significant difference in cluster accessibility to solvent water. For bovine adrenodoxin, containing a 2Fe-2S cluster, and *C. pasteurianum* ferredoxin, containing two 4Fe-4S clusters, exchange against D_2O gives rise to deuterium modulations in the two-pulse echo envelope that are dependent on both protein redox state and incubation time (Orme-Johnson et al., 1983). For reduced Fe-S proteins, this exchange can require as much as 24 h of incubation. With the reduced iron protein from nitrogenase, deuterium exchange is essentially complete within 15 s. The presence of Mg-ATP makes little difference within this time regime (Figure 3). The high degree of Fe-S cluster accessibility to solvent demonstrated by these measurements is consistent with a previously suggested model of Hausinger and Howard (1983), where the metal cluster of the Fe protein is bound between its two subunits.

The experiments of our study suggest that Mg-ATP binds to the iron protein of nitrogenase but not at the iron-sulfur center. The consequence of this is that the interaction of Mg-ATP with the Fe-S cluster is weak, if it exists at all. Interaction of Mg-ATP with the metal center, though, might occur either with an EPR-silent form of the molecule or after association of the iron protein with the iron–molybdenum

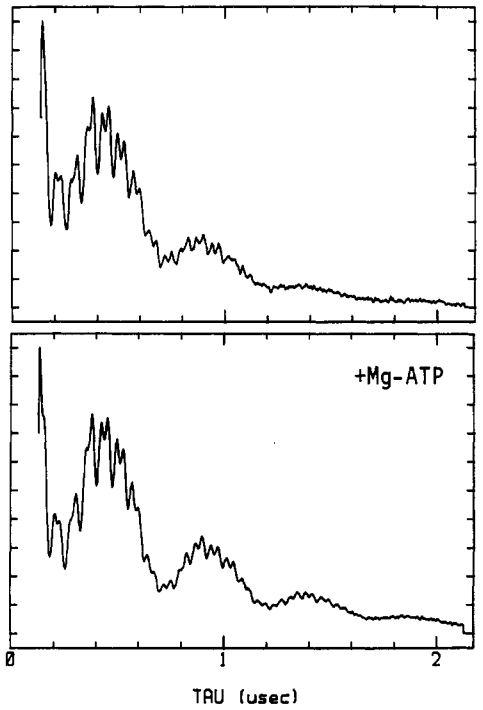

FIGURE 3: Two-pulse ESEEM data for *A. vinelandii* nitrogenase Fe protein exchanged against D_2O in the absence (upper panel) and presence (lower panel) of Mg-ATP. Measurement conditions were microwave frequency, 8.7 GHz; magnetic field strength, 3157 G; microwave pulse power, 50 W; pulse duration, 20 ns (FWHM); sample temperature, 1.8 K; and pulse repetition rate, 200 Hz; each point represents the average of 50 events.

protein. However, EXAFS data do not shown any significant changes in Fe–S bond distance when Mg-ATP is present, providing further evidence that Mg-ATP does not interact directly with the Fe-S center (Lindahl et al., 1987).

REFERENCES

Anderson, G. L., & Howard, J. B. (1984) *Biochemistry 23*, 2118–2122.

Berg, J. M., & Holm, R. H. (1982) in *Iron-Sulfur Proteins* (Spiro, T., Ed.) pp 1–66, Wiley Interscience, New York.

Blumberg, W. E., & Peisach, J. (1974) *Arch. Biochem. Biophys. 162*, 502–512.

Britt, R. D., & Klein, M. P. (1987) *J. Magn. Reson. 74*, 535–540.

Burgess, B. K. (1984) in *Advances in Nitrogen Fixation Research* (Veeger, C., & Newton, W. E., Eds.) pp 103–113, Nijhoff/Junk, The Hague, The Netherlands.

Burgess, B. K., Jacobs, D. J., & Steifel, E. I. (1980) *Biochim. Biophys. Acta 292*, 413–421.

Cammack, R., Chapman, A., McCracken, J., Cornelius, J. B., Peisach, J., & Weiner, J. H. (1988) *Biochim. Biophys. Acta 956*, 307–312.

Dickson, D. P. E., & Cammack, R. (1974) *Biochem. J. 143*, 763–765.

Flanagan, H. L., & Singel, D. J. (1987) *J. Chem. Phys. 87*, 5606–5616.

Gillum, W. O., Mortenson, L. E., Chen, J. S., & Holm, R. H. (1977) *J. Am. Chem. Soc. 99*, 584–595.

Hahn, E. L. (1950) *Phys. Rev. 80*, 580–594.

Hausinger, R. P., & Howard, J. B. (1983) *J. Biol. Chem. 258*, 13486–13492.

Hurst, G. C., Henderson, T. A., & Kreilick, R. W. (1985) *J. Am. Chem. Soc. 107*, 7294–7299.

Lin, C. P., Bowman, M. K., & Norris, J. R. (1985) *J. Magn. Reson. 65*, 369–374.

Lindahl, P. A., Day, E. P., Kent, T. A., Orme-Johnson, W. H., & Münck, E. (1985) *J. Biol. Chem. 260*, 11160–11173.

Lindahl, P. A., Teo, B.-K., & Orme-Johnson, W. H. (1987) *Inorg. Chem. 26*, 3912–3916.

LoBrutto, R., Haley, P. E., Yu, C., & Ohnishi, T. (1987) in *Advances in Membrane Biochemistry and Bioenergetics* (Kim, C. H., Tedeschi, H., Dinan, J. J., & Salerno, J. C., Eds.) pp 449–458, Plenum Press, New York.

Lowry, O. H., Rosebrough, N. J., Fan, A. L., & Randall, R. J. (1951) *J. Biol. Chem. 93*, 265–275.

McCracken, J., Peisach, J., & Dooley, D. M. (1987) *J. Am. Chem. Soc. 109*, 4064–4072.

Mims, W. B. (1972a) *Phys. Rev. B6*, 3543–3545.

Mims, W. B. (1972b) *Phys. Rev. B5*, 2409–2419.

Mims, W. B. (1974) *Rev. Sci. Instrum. 45*, 1583–1591.

Mims, W. B. (1984) *J. Magn. Reson. 59*, 291–306.

Mims, W. B., & Gillen, R. (1967) *J. Chem. Phys. 47*, 3518–3532.

Mims, W. B., & Peisach, J. (1976a) *J. Chem. Phys. 64*, 1074–1091.

Mims, W. B., & Peisach, J. (1976b) *Biochemistry 15*, 3863–3869.

Mims, W. B., & Peisach, J. (1979) in *Biological Applications of Magnetic Resonance* (Shulman, R. G., Ed.) pp 221–269 Academic Press, New York.

Mims, W. B., & Peisach, J. (1981) in *Biological Magnetic Resonance* (Berliner, L. J., & Reuben, J., Eds.) Vol. 3, pp 213–263, Plenum Press, New York.

Mortenson, L. E. (1972) *Methods Enzymol. 29*, 446–456.

Nakos, G., & Mortenson, L. E. (1971) *Biochemistry 10*, 455–458.

Orme-Johnson, W. H. (1985) *Annu. Rev. Biophys. Chem. 14*, 419–459.

Orme-Johnson, N. R., Mims, W. B., Orme-Johnson, W. H., Bartsch, R. G., Cusnovich, M. A., & Peisach, J. (1983) *Biochim. Biophys. Acta 748*, 68–72.

Orme-Johnson, W. H., Hamilton, W. D., Ljones, T., Tso, M. Y., Burris, R. H., Shah, V. K., & Brill, W. J. (1972) *Proc. Natl. Acad. Sci. U.S.A. 69*, 3142–3145.

Orme-Johnson, W. H., Davis, L. C., Henzl, M. T., Averill, B. A., Orme-Johnson, N. R., Münck, E., & Zimmerman, R. (1977) in *Recent Developments in Nitrogen Fixation* (Newton, W., Prostgate, J. R., & Rodriguez-Barrauco, C., Eds.) pp 131–178, Academic Press, New York.

Peisach, J., & Mims, W. B. (1973) *Proc. Natl. Acad. Sci. U.S.A. 70*, 2979–2982.

Peisach, J., & Mims, W. B. (1976) *Chem. Phys. Lett. 37*, 307–310.

Peisach, J., Orme-Johnson, N. R., Mims, W. B., & Orme-Johnson, W. H. (1977) *J. Biol. Chem. 252*, 5643–5650.

Peisach, J., Beinert, H., Emptage, M. H., Mims, W. B., Fee, J. A., Orme-Johnson, W. H., Rendina, A. R., & Orme-Johnson, N. R. (1983) *J. Biol. Chem. 258*, 13014–13016.

Smith, B. E., & Lang, G. (1974) *Biochem. J. 137*, 169–180.

Stephens, P. J., McKenna, C. E., Smith, B. E., Nguyen, H. T., McKenna, M. C., Thompson, A. J., Devlin, F., & Jones, J. B. (1979) *Proc. Natl. Acad. Sci. U.S.A. 76*, 2585–2589.

Stephens, P. J., McKenna, C. E., McKenna, M. C., Nguyen, H. T., & Sowe, D. J. (1982) in *Electron Transport and Oxygen Utilization* (Chien Ho, Ed.) pp 405–409, Elsevier North-Holland, New York.

Thompson, C. L., Johnson, C. E., Dickson, D. P. E., Cammack, R., Hall, D. O., Weser, U., & Rao, K. K. (1974) *Biochem. J. 139*, 97-103.
Thorneley, R. N. F., Lowe, D. J., Eady, R. R., & Miller, R. W. (1979) *Biochem. Soc. Trans. 7*, 633-636.
Tsukihara, T., Fukuyama, K., Nakamura, T., Katsube, Y., Tanaka, N., Kukudo, Wada, M. K., Hase, T., & Matsubara, H. (1981) *J. Biochem. 90*, 1763-1773.
Walker, G., & Mortensen, L. E. (1973) *Biochem. Biophys. Res. Commun. 53*, 904-909.
Zumft, W. G., Palmer, G., & Mortenson, L. E. (1973) *Biochim. Biophys. Acta 292*, 413-421.
Zumft, W. G., Mortenson, L. E., & Palmer, G. (1974) *Eur. J. Biochem. 46*, 525-536.

Human Plasma Fibronectin Structure Probed by Steady-State Fluorescence Polarization: Evidence for a Rigid Oblate Structure†

Michael J. Benecky,* Carl G. Kolvenbach,‡ Richard W. Wine, James P. DiOrio, and Michael W. Mosesson

Sinai Samaritan Medical Center, University of Wisconsin Medical School, Milwaukee Clinical Campus, Milwaukee, Wisconsin 53233

Received September 29, 1989; Revised Manuscript Received November 20, 1989

ABSTRACT: In order to more clearly define the structure of human plasma fibronectin (PFn) under physiologic buffer conditions, we determined the mean harmonic rotational relaxation times (ρ_H) of PFn and the thrombin-derived 190/170-kDa PFn fragment using steady-state fluorescence polarization. These measurements utilized the long lifetime emission ($\tau = 1.2 \times 10^{-7}$ s) exhibited by 1-pyrenebutyrate, which had been covalently attached to amino groups at random sites on the PFn subunit. Our data analysis assumed that two independent processes depolarize the fluorescence exhibited by the dansylcadaverine and 1-pyrenebutyrate conjugates of PFn: (A) rapid ($\rho_H < 10^{-9}$ s) "thermally-activated" localized rotational motion of the protein side chains bearing the fluorescent probe [Weber, G. (1952) *Biochem. J. 51*, 145-154] and (B) slow ($\rho_H \sim 10^{-6}$ s) temperature-independent global rotational motion of the whole PFn molecule. Since only the ρ_H associated with the latter process is a true hydrodynamic parameter (i.e., sensitive to size and/or shape of the PFn molecule), we utilized isothermal polarization measurements to discriminate against the interfering signal arising from "thermally activated" probe rotation. The ρ_H (4.4 ± 0.9 μs) derived from an experiment in which pyrene–PFn fluorescence polarization was monitored as a function of sucrose concentration at constant temperature is 7 (±1.4) times longer than that predicted for an equivalent hydrated sphere. We propose that "thermally activated" probe rotation gives rise to the nearly 100-fold shorter PFn ρ_H values previously reported in the literature. Consequently, our data exclude all previous models which invoke segmental flexibility of the PFn peptide backbone. The simplest hydrodynamic model supported by our fluorescence data is an oblate ellipsoid with an axial ratio of 15:1. All prolate models can be unambiguously excluded by this result. We estimate that the disk-shaped PFn molecule has a diameter and thickness of 30 and 2 nm, respectively. Electron microscopy of negatively stained PFn specimens on carbon also showed PFn to have a compact rounded structure. The much faster rotational relaxation rate of the pyrene–190/170-kDa PFn fragment ($\rho_H = 0.92 \pm 0.11$ μs) compared to pyrene–PFn indicated that this monomeric PFn fragment, like native PFn, had an oblate shape under physiologic buffer conditions.

Plasma fibronectin (PFn)[1] is a 520-kDa (Rocco et al. 1987; Sjöberg et al., 1987) heterodimeric glycoprotein which mediates cell attachment and spreading in a wide variety of biological systems. The molecular basis for this adhesive biological activity resides in its multiple binding affinities for various macromolecules found within cells, on cell surfaces, and in extracellular matrices. Although PFn has been characterized by a wide variety of biophysical techniques [for reviews, see Hermans (1985) and Odermatt and Engel (1989)], the relationship between PFn structure and its various adhesive biological functions remains poorly understood. Furthermore, these previous biophysical studies have not yet

† This investigation was supported by NHLBI Program Project Grant HL-28444. An abstract of this work was presented at the American Society for Cell Biology and the American Society for Biochemistry and Molecular Biology Joint Meeting, January 29–February 2, 1989, San Francisco, CA (Benecky et al., 1988b).

* Address correspondence to this author at the Sinai Samaritan Medical Center, Winter Research Institute, 836 North Twelfth St., Milwaukee, WI 53233.

‡ Present address: Amgen Corp., 1900 Oak Terrace Lane, Thousand Oaks, CA 91320.

[1] Abbreviations: PFn, human plasma fibronectin; ρ_H, mean harmonic rotational relaxation time; TBS, Tris-buffered saline (50 mM Tris-HCl/150 mM NaCl, pH 7.4, buffer); EDTA, ethylenediaminetetraacetic acid; PMSF, phenylmethanesulfonyl fluoride; KIU, kallikrein inactivator unit(s); SDS, sodium dodecyl sulfate; SDS–PAGE, sodium dodecyl sulfate–polyacrylamide gel electrophoresis, τ, fluorescence lifetime; PBS, phosphate-buffered saline (30 mM sodium phosphate/100 mM NaCl, pH 7.4, buffer); $\langle\tau\rangle$, second-order average fluorescence lifetime; η, solvent viscosity; ρ_o, rotational relaxation time expected for an equivalent hydrated sphere; pyrene–PFn, 1-pyrenebutyrate-conjugated PFn; CD, circular dichroism; STEM, scanning transmission electron microscopy; ANS–PFn, 1-anilino-8-naphthalenesulfonate-conjugated PFn.

0006-2960/90/0429-3082$02.50/0